Analysis on Accuracy of Charge-Pumping Measurement with Gate Sawtooth Pulses

P. T. Lai, J. P. Xu, C. K. Poek, and Y. C. Cheng, *Member, IEEE*

***Abstract*— Charge-pumping (CP) measurement is performed on MOSFET's with their gates tied to sawtooth pulses. Influence of both rise time (t_r) and fall time (t_f) on the CP current of the devices with different channel lengths is investigated at different pulse frequencies. Results show that the dominant mechanism affecting the measurement accuracy is the energy range of interface-trap distribution $D_{\mathrm{it}}(E)$ swept by the gate signal for frequencies below 500 kHz and carrier emission for frequencies above 500 kHz. For frequencies higher than 600 kHz, incomplete recombination could be an additional mechanism when t_f is too short. Hence, it is suggested that low frequency is more favorable than high frequency, especially for sawtooth pulses with long t_r and short t_f, due to little carrier emission and negligible geometric effects even for devices as long as 50 μm. However, if high frequency (e.g., 1 MHz) is required to obtain a sufficiently large S/N ratio in the CP current, sawtooth pulses with equal t_r and t_f should be chosen for the least carrier emission effect and thus more reliable results on interface-state density. Moreover, for both sawtooth and trapezoidal pulses with a typical amplitude of 5 V, a lower limit of 200 ns for t_r and t_f is necessary to suppress all the undesirable effects in devices shorter than at least 20 μm.**

***Index Terms*— Charge carrier processes, MOSFET's, silicon materials/devices.**

I. INTRODUCTION

THE charge-pumping (CP) technique is a well-known experimental approach for assessing the interface-state density D_{it} of MOSFET's [1], [2]. Using this technique, it has been possible to measure the spatial variation of hot-carrier-induced Dit near the drain [3]–[5]. The pulses applied to the gate of the MOSFET can be square, triangular or sawtooth waves. A strong dependence of the charge-pumping current (I_{CP}) on the shape of the gate pulses was observed [1], [2]. It was found that a geometric component in I_{CP} [1], [6] leading to an unacceptable over-estimation of D_{it} happened especially for long-channel devices when square pulses with short rise/fall times were used. However, this geometric component could be suppressed by using sawtooth pulses because of the longer rise/fall times available for the mobile carriers to reach source/drain when driving the surface back to accumulation [1], [2]. Hence, it is believed that the sawtooth pulse has high potential in accurate estimation of D_{it}. However, different rise/fall times which are dependent on frequencies and shapes of the sawtooth pulses would also result in different I_{CP} and thus different D_{it}, which is hardly discussed in the literature. This work aims to carry out some investigations on this aspect to determine the most suitable shape of the sawtooth pulse at different frequencies which could give the least error in CP measurement.

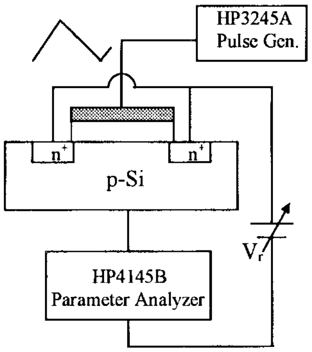

Fig. 1. Schematic diagram of the setup for CP measurement.

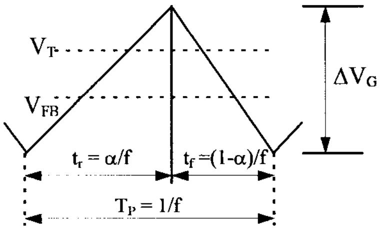

Fig. 2. Definitions of rise time (t_r), fall time (t_f) and the fraction of one pulse period when the gate voltage is rising (α) for a sawtooth pulse.

II. EXPERIMENTAL

The basic setup for CP measurement is shown in Fig. 1. An HP3245A pulse generator is used to supply the gate sawtooth pulses, and a reverse bias of 0.1 V is applied to the source and the drain of a MOSFET. The substrate current of the device (I_{CP}) is measured by an HP4145B parameter analyzer with varying pulse base level to drive the silicon surface from accumulation to inversion while keeping the amplitude of the pulse constant ($\Delta V_G = 5$ V). Definitions of rise time (t_r) and fall time (t_f) of the sawtooth pulses are presented in Fig. 2, where f is the pulse frequency and α is defined as the fraction of the period where the gate voltage is rising. Frequencies of 100 kHz–1 MHz are used in measurement with $\alpha = 0.1$, 0.3, 0.5, 0.7, and 0.9. The samples are nMOSFET's with thermally grown gate oxide (thickness: 200 Å). Different channel lengths

---

Manuscript received April 30, 1997; revised September 29, 1997. The review of this paper was arranged by Editor D. P. Verret. This work was supported in part by the RGC and CRCG Research Grants, the University of Hong Kong.

P. T. Lai, C. K. Poek, and Y. C. Cheng are with the Department of Electrical and Electronic Engineering, the University of Hong Kong, Hong Kong.

J. P. Xu is with the Department of Solid State Electronics, Huazhong University of Science and Technology, Wuhan 430074, China.

Publisher Item Identifier S 0018-9383(98)02297-7.

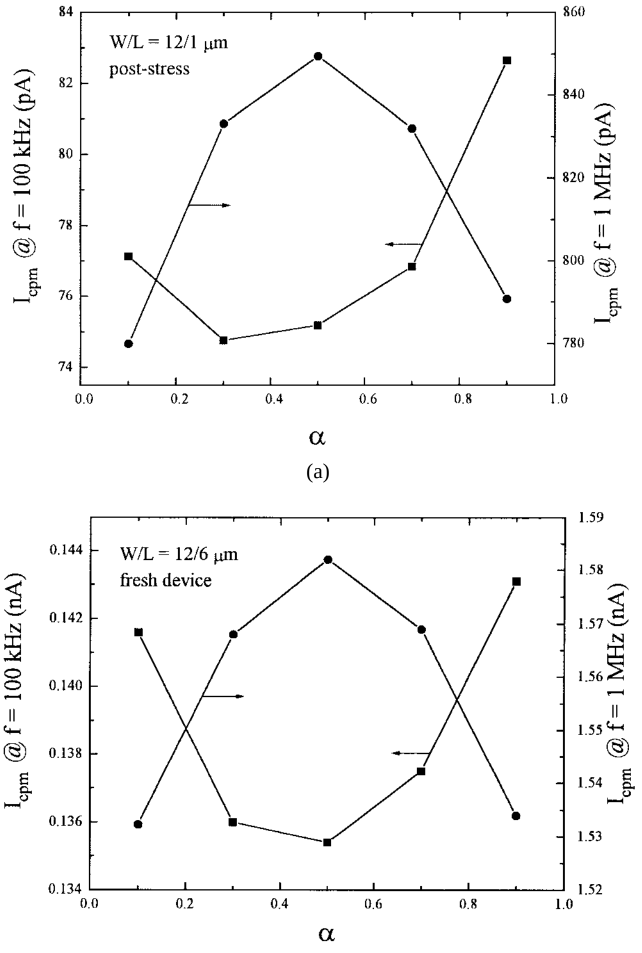

(a)

(b)

Fig. 3. Variation of maximum CP current (I_{CPm}) with α for pulse frequency $f = 100$ kHz and 1 MHz, respectively. (a) $W/L = 12/1$ μm, after stress of $V_D = 2V_G = 7$ V for 1000 s and (b) $W/L = 12/6$ μm, fresh device.

($L = 1$, 6, 20, and 50 μm) are used to examine the validity of estimating D_{it} when gate sawtooth pulses are used, while the geometric effect is checked by means of trapezoidal pulses with different t_r and t_f.

III. RESULTS AND DISCUSSION

Fig. 3 shows the change of maximum charge-pumping current (I_{CPm}) with α for different pulse frequencies and device channel lengths. It can be seen that I_{CPm} exhibits opposite variation trend for $f = 100$ kHz and 1 MHz. I_{CPm} for $f = 100$ kHz is minimum but for $f = 1$ MHz is maximum at around $\alpha = 0.5$, i.e., $I_{\mathrm{CPm}}(\alpha)$ curve changes from U-shape at 100 kHz to bell-shape at 1 MHz. The mechanism behind this phenomenon could be explained by considering the following time constants.

According to the discussion in [2], there are six different processes during one cycle of the gate pulse, among which the nonsteady-state emissions of holes from the interface states to the valence band at the rising edge of the gate pulse and electrons from the interface states to the conduction band at the falling edge result in a decrease in I_{CP}. The corresponding emission times for electrons and holes can be expressed as [2]

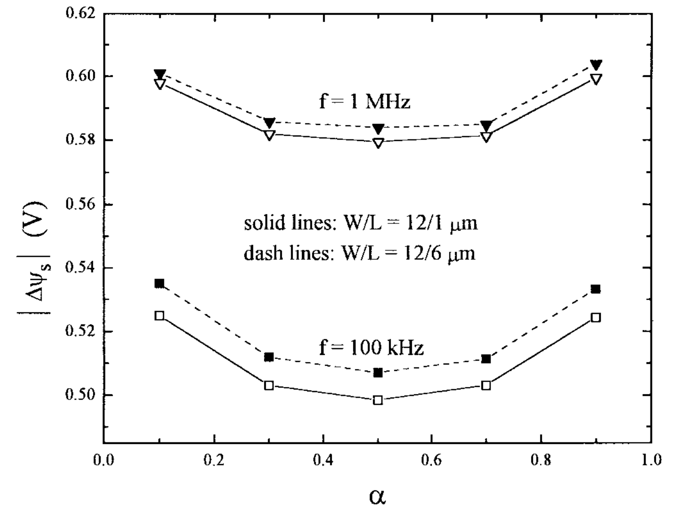

Fig. 4. Surface potential $\Delta\psi_s$ as a function of α for different frequencies and channel lengths.

$$t_{em,e} = \frac{|V_{\mathrm{FB}} - V_T|}{\Delta V_G} \cdot \frac{1}{f}(1-\alpha) \tag{1}$$

$$t_{em,h} = \frac{|V_{\mathrm{FB}} - V_T|}{\Delta V_G} \cdot \frac{1}{f} \cdot \alpha \tag{2}$$

where V_{FB} and V_T are the flatband voltage and the threshold voltage, respectively. By determining V_T and V_{FB} from 75% of I_{CPm} at the rising edge and 25% of I_{CPm} at the falling edge of I_{CP}, respectively, $t_{em,e}$ and $t_{em,h}$ can be estimated. It is found that $t_{em,e}/t_{em,h}$ decreases/increases as α increases, while electron and hole emissions seem to be dominant, respectively, for $\alpha = 0.1$ and 0.9 due to their longer emission times (see Table I).

When the gate voltage is close to V_T at the rising edge or V_{FB} at the falling edge, the trapping time constants of electrons (τ_e) or holes (τ_h) become respectively important, which can be approximately given by [1]

$$\tau_{e,h} = \frac{1}{V_{\mathrm{th}}\sigma_{n,p}n_s} \tag{3}$$

where ν_{th} is the thermal velocity of carriers, $\sigma_{n,p}$ are the capture cross sections of electron and hole and n_s is the surface concentration of carriers. With $n_s = 10^{16}$ cm^{-3} as extracted from C-V measurements, $\nu_{\mathrm{th}} = 107$ cm/s, $\sigma_n = 6.5 \times 10^{-16}$ cm^2 and $\sigma_p = 2.4 \times 10^{-16}$ cm^2 [7], τ_e and τ_h can be estimated to be about 15 and 42 ns, respectively. The times available for electron or hole capture (t_{ce} or t_{ch}) can also be estimated simply from Fig. 2. t_{ce} includes the total time when $V_G \geq V_T$ at both the rising and falling edges of the gate pulse signal, while t_{ch} is the total time when $V_G \leq V_{\mathrm{FB}}$ only at the falling edge. So, for different frequencies and α, t_{ce} and t_{ch} can be calculated as shown in Table I.

From Table I, it can be clearly seen that electrons can be trapped in a very short time, and thus electron filling of interface traps should be complete even for $\alpha = 0.1$ at $f = 1$ MHz. However, hole filling of the traps during t_f is probably incomplete because of $\tau_h > t_{\mathrm{ch}}$ when $\alpha = 0.9$ at $f = 1$

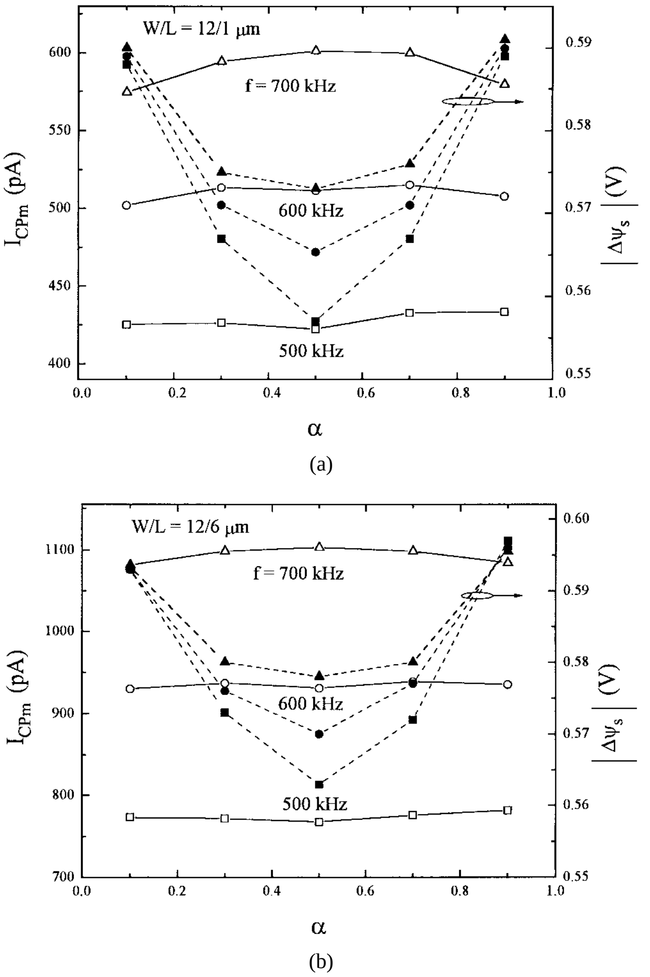

Fig. 5. Variations of maximum CP current ($I_{\rm CPm}$) and surface potential $\Delta\psi_s$ with α for $f = 500$, 600 and 700 kHz. (a) $W/L = 12/1$ μm, and (b) $W/L = 12/6$ μm.

MHz. On the other hand, the larger the α, the smaller/larger is the effect of electron/hole emission on $I_{\rm CP}$. As a result, there will be more electron and hole emissions which reduce recombination due to longer emission time ($t_{em,e}/t_f$ and $t_{em,h}/t_r$ are close to 50%), and thus $I_{\rm CP}$ is smaller. For $\alpha = 0.5$ at 1 MHz, the least emission and maximum recombination occur due to the relatively shorter electron and hole emission times ($t_{em,e}/t_f$ and $t_{em,h}/t_r$ decrease to ~40%), resulting in largest $I_{\rm CP}$. However, for a lower frequency of 100 kHz, $I_{\rm CPm}$ variation with α basically follows the trend of the surface-potential sweep $\Delta\psi_s = (E_{em,e} - E_{em,h})/q$ [2], with $E_{em,e}$ and $E_{em,h}$ being the energy positions where electron and hole emissions cease, respectively. Taking into account the carrier emissions [2]

$$\Delta\psi_s = \frac{2kT}{q} \ln\left[\nu_{\rm th} n_i \sqrt{\sigma_n \sigma_p} \sqrt{\alpha(1-\alpha)} \frac{1}{f} \frac{|V_{\rm FB} - V_T|}{|\Delta V_G|}\right]. \tag{4}$$

Setting $\partial\Delta\psi_s/\partial\alpha = 0$, it can be found that when $\alpha = 0.5, |\Delta\psi_s|$ has indeed the minimum value, as depicted in Fig. 4. Since $I_{\rm CP}$ is proportional to $D_{\rm it}, f$ and $\Delta\psi_s$ [2]

$$I_{\rm CP} = q^2 f W L D_{\rm it} \Delta\psi_s. \tag{5}$$

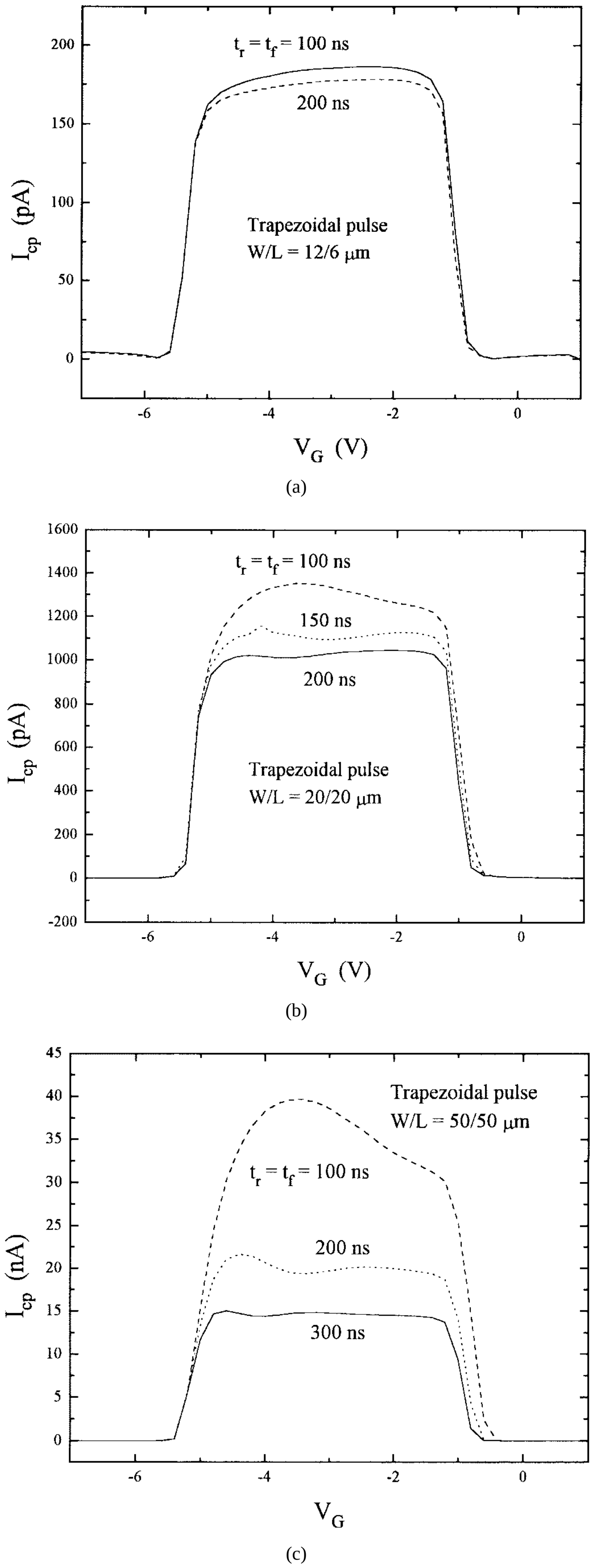

Fig. 6. CP curves measured by trapezoidal pulses at 100 kHz with different t_r and t_f for devices with different channel lengths. (a) $W/L = 12/6$ μm, (b) $W/L = 20/20$ μm and (c) $W/L = 50/50$ μm.

TABLE I
THE ESTIMATED VALUES FOR VARIOUS TIME CONSTANTS

f	α	$t_{em,e}$ (ns)	$t_{em,h}$ (ns)	t_{ce} (ns)	t_{ch} (ns)	τ_e (ns)	τ_h (ns)
	0.1	1720	190	2500	2250	15	42
100 kHz	0.5	970	970	2500	1250	15	42
	0.9	185	1670	2500	250	15	42
	0.1	450	50	250	225	15	42
1 MHz	0.5	202	202	250	125	15	42
	0.9	47	430	250	25	15	42

$\Delta\psi_s$ variation with α should primarily be responsible for the $I_{\rm CPm}$ variation with $f = 100$ kHz due to shorter electron and hole emission times ($t_{em,e}/t_f$ and $t_{em,h}/t_r$ are only ~19%). In fact, from 100 kHz to 1 MHz, the $I_{\rm CPm}$ variation undergoes a progressive transition, with a transition frequency somewhere in 500–700 kHz. As shown in Fig. 5, for 500 kHz, the dominance of $\Delta\psi_s$ on $I_{\rm CPm}$ is greatly weakened by the carrier emission processes at around $\alpha = 0.1$ and 0.9. When f is increased to 600 kHz, the effects of carrier emission become further stronger at the two ends and obviously dominant for $f = 700$ kHz. Physically, as long as the rate of change of trapped charge density (Q_t) as imposed by the carrier emission $(dQ_t/dt|_{\rm em})$ is larger than the rate of change of trapped charge density required to maintain steady-state condition $(dQ_t/dt|_{\rm ss})$, the channel is in steady-state condition [8]. Since $dQ_t/dt|_{\rm ss} \propto d\psi_s/dt \propto f$ [2], the demand of $dQ_t/dt|_{\rm em} > dQ_t/dt|_{\rm ss}$ is readily met at low frequencies, and thus it is possible to keep the trap occupation in dynamic equilibrium with the voltage sweep. This is why $I_{\rm CPm}(\alpha)$ and $\Delta\psi_s(\alpha)$ have the similar behavior at $f = 100$ kHz. However, as f increases to 1 MHz, $d\psi_s/dt$ and thus $dQ_t/dt|_{\rm ss}$ increase by a factor of 10 and so it is difficult to maintain the channel in steady-state regime for a large part of t_r and t_f, especially for α around 0.1 or 0.9. Hence, the carrier emission effect increases and $I_{\rm CPm}(\alpha)$ becomes like that in Fig. 3, instead of like $\Delta\psi_s(\alpha)$. Moreover, it is interesting to note that when $\alpha = 0.9$ at 600 kHz, $t_f \approx 167$ ns which gives a $t_{\rm ch}$ of 42 ns, equal to the estimated hole trapping time in Table I. This implies that when $t_f < 167$ ns, incomplete recombination at the falling edge would occur. From the results in Fig. 5 and the above discussion, it is reasonable to take 500 kHz as a critical frequency under which the effects of carrier emission under long t_r or t_f and incomplete recombination under short t_f on $I_{\rm CP}$ can be ignored, resulting in a lower limit of 200 ns for t_r and t_f with $\Delta V_G = 5$ V.

Fig. 3 shows that $I_{\rm CPm}$ at $\alpha = 0.9$ is always slightly larger than the one at $\alpha = 0.1$ for both 100 kHz and 1 MHz although they have almost the same $\Delta\psi_s$ as calculated in Fig. 4. There are two possible reasons: 1) the geometric effect at $\alpha = 0.9$; and 2) the carrier emission effect with electron emission at $\alpha = 0.1$ more than hole emission at $\alpha = 0.9$, which is supported by their different emission times $(t_{em,e} > t_{em,h})$.

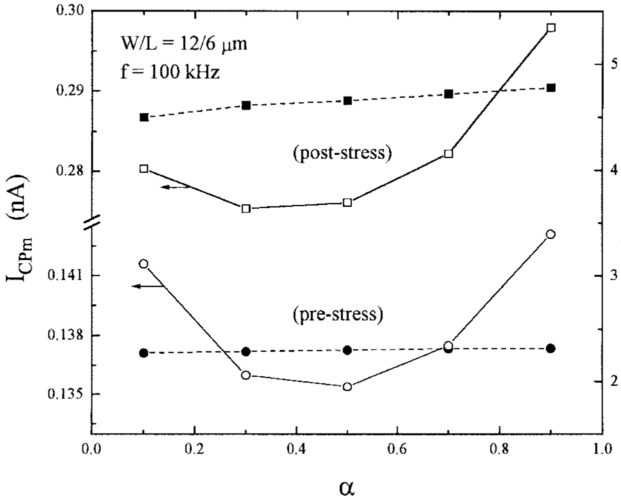

Fig. 7. Measured $I_{\rm CPm}$ and $D_{\rm it}$ for a transistor with $W/L = 12/6$ μm before and after stress ($V_D = 2V_G = 7$ V for 1000 s). Pulse frequency is 100 kHz. It can be seen that the larger the $D_{\rm it}$, the larger is the electron emission effect at $\alpha = 0.1$ than the hole emission effect at $\alpha = 0.9$.

Since $I_{\rm CPm}$ of the 1-μm device (which should hardly has any geometric effect) exhibits a trend similar to that of the 6-μm device and the CP curves of the latter measured by trapezoidal pulses with the same t_f of 100 ns do not show any geometric effect [see Fig. 6(a)], the carrier emission effect should be dominant. Furthermore, the larger the $D_{\rm it}$ in the device, the more obvious the carrier emission effect seems to be, due to the fact that the difference between the $I_{\rm CPm}$'s of the 6-μm device at $\alpha = 0.1$ and 0.9 increases from 2 pA before stress to 18 pA after stress ($V_D = 2V_G = 7$ V for 1000 s), as shown in Fig. 7. This is also reflected from the 1-μm device in Fig. 3(a) which has gone through the same stress in order to produce a measurable $I_{\rm CP}$. However, for devices with longer channel, the geometric effect should play a role, based on the results shown in Fig. 8, where the difference between $I_{\rm CPm}$'s at $\alpha = 0.9$and 0.1 with $f = 1$ MHz increases from 0.17 pA per μm width for the 6-μm fresh device to 1 for the 20-μm fresh device and 300 for the 50-μm fresh device. The hump in the saturation region of Fig. 6(b) and (c) for $t_f = 100$ ns also indicates the geometric effect [2]. So, it can be proposed that the combined effects of the geometric component and carrier emission for $\alpha = 0.9$ ($t_f = 100$ ns) and the carrier emission effect for $\alpha = 0.1$ ($t_f = 900$ ns) result in a larger $I_{\rm CPm}$ difference for the long-channel devices. More significantly, Fig. 6(b) and (c) illustrate that the geometric effect is negligible if t_f longer than 150 ns for the 20-μm device and 300 ns for the 50-μm device. This demonstrates that the lower limit of 200 ns for t_r and t_f derived above is also greatly favorable in eliminating the geometric effect for L shorter than at least 20 μm and $I_{\rm CP}$ measured by sawtooth pulses at a low frequency of 100 kHz should hardly have any geometric component even for $\alpha = 0.9$ due to a long t_f of 1 μs.

The above discussions have shown that the carrier emission effect is highly sensitive to f. For $f = 100$ kHz, its effect is fully displayed in $\Delta\psi_s$ due to relatively long t_r and t_f, and low $d\psi_s/dt$, resulting in different $\Delta\psi_s$ for different α, as shown

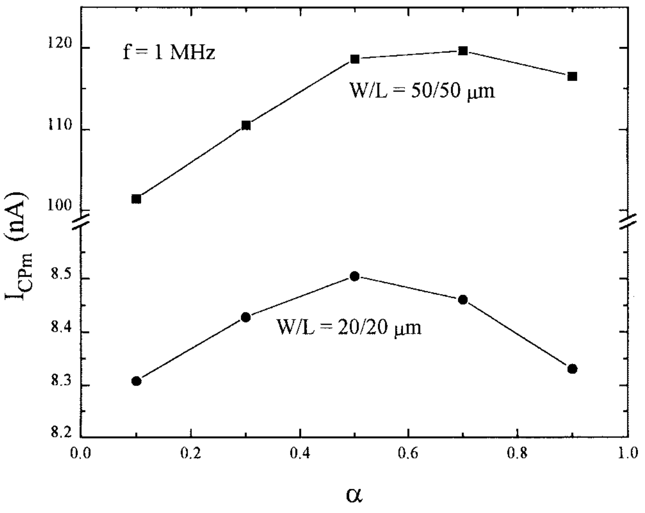

Fig. 8. Maximum CP current (I_{CPm}) variations of two long-channel devices with α for a pulse frequency of 1 MHz. It can be seen that the geometric effect distinctly appears at around $\alpha = 0.9$.

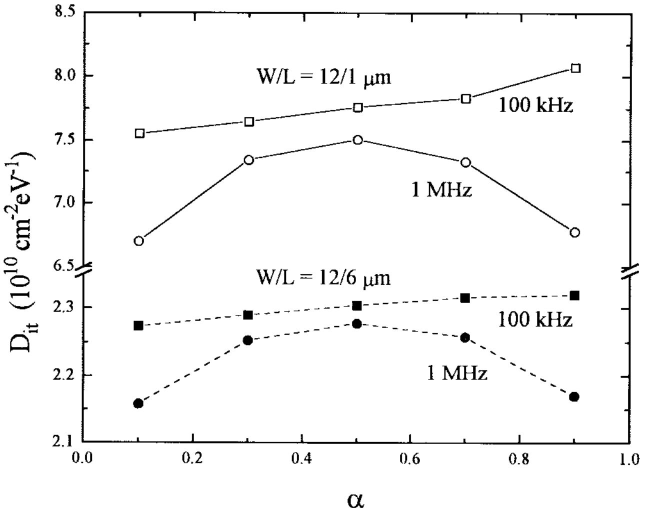

Fig. 9. Measured D_{it} under different f and α for two devices with $W/L = 12/1$ and 12/6 μm, respectively.

in Fig. 4. Therefore, the measured D_{it} at different α as shown in Fig. 9 should correspond to interface-state density averaged over different energy range of $D_{\mathrm{it}}(E)$. Since interface traps have a U-shape distribution in the band gap with a flat region covering an energy range of ~0.56 eV near midgap [9], α should be set at ~0.9 for a low frequency around 100 kHz with $\Delta\psi_s \approx 0.53$ eV from Fig. 4 in order to sweep an energy range as wide as possible and thus characterize the interface-state density more accurately. For high frequencies (e.g., 1 MHz), since the carrier emission effect is larger than that at low frequency, all the measured D_{it} at different α are smaller, with the value at $\alpha = 0.5$ closest to that measured with $f = 100$ kHz due to the least carrier emission effect. Therefore, when sawtooth gate pulses are used to measure D_{it}, low frequency and short t_f (dependent on the signal generator used, in our case, maximum $\alpha = 0.95$, giving a minimum $t_f = 500$ ns for 100 kHz) are suitable. If frequencies higher than 500 kHz are employed for obtaining a larger I_{CP} in noisy situations, α should be set at around 0.5.

IV. SUMMARY

Influence of rise time t_r and fall time t_f of sawtooth pulses on the CP current of MOSFET's with different channel lengths is investigated for different pulse frequencies. It is found that the geometric component of the CP current can be ignored for channels shorter than at least 6 μm under a high pulse frequency of 1 MHz, and for even longer channels under lower frequencies. Main mechanisms affecting measurement accuracy are attributed to the energy range of interface traps swept for low frequencies (below 500 kHz) and carrier emission for high frequencies (above 500 kHz), with the effect of electron emission overwhelming that of hole emission. For frequencies higher than 600 kHz, incomplete recombination could also occur for $t_f < 167$ ns. As a result, 5-V sawtooth or trapezoidal pulses with 200-ns t_r and t_f are demonstrated to be efficient in suppressing the carrier emission, incomplete recombination and geometric effects for devices shorter than at least 20 μm. Therefore, low-frequency pulses around 100 kHz with long t_r and short t_f are preferred to obtain $D_{\mathrm{it}}(E)$ over a wider energy range and decrease the electron emission effect. If high frequency has to be used to enhance the I_{CP} signal, pulses with the same t_r and t_f can result in the least carrier emission effect and thus more accurate D_{it} value.

REFERENCES

[1] J. S. Brugler and P. G. A. Jespers, "Charge pumping in MOS devices," *IEEE Trans. Electron Devices*, vol. ED-16, pp. 297–302, 1969.

[2] G. Groeseneken, H. E. Maes, N. Beltran, and R. F. de Keersmaecker, "A reliable approach to charge-pumping measurements in MOS transistors," *IEEE Trans. Electron Devices*, vol. ED-31, pp. 42–53, 1984.

[3] T. Poorter and P. Zoestbergen, "Hot carrier effects in MOS transistors," in *IEDM Tech. Dig.*, 1984, pp. 100–103.

[4] M. G. Ancona, N. S. Saks, and D. McCarthy, "Lateral distribution of hot-carrier-induced interface traps in MOSFET's," *IEEE Trans. Electron Devices*, vol. 35, pp. 2221–2228, 1988.

[5] W. Chen, A. Balasinski, and T. P. Ma, "Lateral profiling of oxide charge and interface traps near MOSFET junctions," *IEEE Trans. Electron Devices*, vol. 40, pp. 187–196, 1993.

[6] T. Ouisse, S. Cristoloveanu, T. Elewa, H. Haddara, G. Borel, and D. E. Ioannou, "Adaptation of the charge pumping technique to gated p-i-n diodes fabricated on silicon on insulator," *IEEE Trans. Electron Devices*, vol. 38, pp. 1432–1444, 1991.

[7] H. Seghir, S. Cristoloveanu, R. Jerisian, J. Oualid, and A.-J Auberton-Herve, "Correlation of the leakage current and charge pumping in silicon on insulator gate-controlled diodes," *IEEE Trans. Electron Devices*, vol. 40, pp. 1104–1110, 1993.

[8] J. G. Simmons and L. S. Wei, "Theory of dynamic charge current and capacitance characteristics in MIS system containing distributed surface traps," *Solid-State Electron.*, vol. 16, p. 53, 1973.

[9] M. H. While and J. R. Cricchi, "Characterization of thin-oxide NMOS memory transistors," *IEEE Trans. Electron Devices*, vol. ED-19, p. 1280, 1972.

P. T. Lai, for photograph and biography, see p. 528 of the February 1998 issue of this TRANSACTIONS.

J. P. Xu, for photograph and biography, see p. 528 of the February 1998 issue of this TRANSACTIONS.

C. K. Poek received the B. Eng. degree from the Department of Electrical and Engineering, the University of Hong Kong, in 1997.

Currently, he is an Electronic Engineer at S. Megga Technology, Ltd., Hong Kong.

Y. C. Cheng (M'78), for photograph and biography, see p. 528 of the February 1998 issue of this TRANSACTIONS.